ACS OMEGA

http://pubs.acs.org/journal/acsodf

Article

Efficient Fluoride Removal by a Fixed-Bed Column of Self-Assembled Zr(IV)-, Fe(III)-, Cu(II)-Complexed Polyvinyl Alcohol Hydrogel Beads

Sai Kiran Mani and Rajni Bhandari*

Cite This: *ACS Omega* 2022, 7, 15048−15063

Read Online

ACCESS | Metrics & More | Article Recommendations

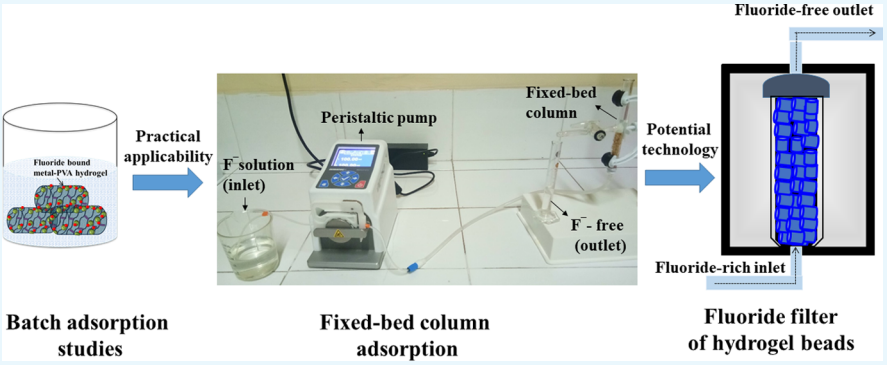

ABSTRACT: Fixed-bed column adsorption studies are performed with metal-complexed polyvinyl alcohol (PVA) hydrogel beads to remove fluoride from groundwater. The fixed-bed column (bed height = 8 ± 0.2 cm) of copper−zirconium−PVA (PCZH), zirconium−PVA (PZH), and iron−zirconium−PVA (PFZH) hydrogel beads have equilibrium fluoride removal capacities of 17.26 ± 0.05, 31.67 ± 0.05, and 11.84 ± 0.05 mg g^{-1} from a 10 ± 0.20 mg L^{-1} fluoride solution of pH 6.5 maintained at a flow rate of 1 ± 0.01 mL min^{-1}. The breakthrough curves for fluoride adsorption are analyzed by non-linear empirical models of Thomas, Bohart−Adams, Yoon−Nelson, and semi-empirical bed depth service time models. The maximum fluoride adsorption capacities obtained from the Thomas model are 25.66 ± 0.05, 38.17 ± 0.05, and 13.75 ± 0.05 mg g^{-1} for PCZH, PZH, and PFZH. Moreover, the column of PZH (bed height = 4 ± 0.2 cm) removes about 1.67 ± 0.05 mg g^{-1} of fluoride from the alkaline groundwater sample with high total dissolved solids containing 2.84 ± 0.20 mg L^{-1} fluoride maintained at a flow rate of 0.5 ± 0.01 mL min^{-1}. The fluoride removal efficiency decreases marginally (<1 ± 0.02%) in the presence of interfering ions such as chlorides, sulfates, phosphates, bicarbonates, and nitrates. Furthermore, the fixed-bed column (bed height = 4 ± 0.2 cm) of PCZH, PZH, and PFZH remove 7.40 ± 0.05, 14.85 ± 0.05, and 6.53 ± 0.05 mg g^{-1} fluoride, respectively, even after the third regeneration cycle. Additionally, the hydrogel beads are effective in the removal of arsenate (≤90 ± 0.02%) and chromate ions (≤96 ± 0.02%) from 100 ± 0.20 mg L^{-1} solution in batch adsorption studies. Therefore, the hydrogel beads could be used as potent filters for the removal of fluoride, chromate, and arsenate ions from water.

1. INTRODUCTION

Groundwater is widely used for domestic needs. However, the presence of high fluoride content in groundwater is a matter of concern. Earth's crust has about 625 mg kg^{-1} of fluoride, which is mainly present in minerals such as fluorite, topaz, cryolite, amphiboles, sellaite, apatite, villiaumite, mica, and certain clays.[1] The concentration of fluoride in groundwater also depends on lithology, residence time, seasonal changes, and local pollution caused mainly by anthropogenic sources such as industries, oil refineries, coal burning, or leakages in the aquifers.[1,2] Fluoride contamination of groundwater is a global issue affecting several million populations of Asia, Africa, and United States of America.[3]

In India, fluoride contamination is rampant in the southern and western regions encompassing the districts of Andhra Pradesh, Telangana, Kerala, Uttar Pradesh, Uttarakhand, Bihar, Jharkhand, and West Bengal. The fluoride concentration in groundwater varies from 0.6 to 7.8 mg L^{-1} in these regions.[1,2,4]Dfig6 The permissible limit of fluoride in drinking

Received: February 10, 2022
Accepted: April 5, 2022
Published: April 20, 2022

Table 1. Summary of Material Characteristics and Outcomes of Batch Fluoride Adsorption Studies of the Hydrogel Beads[18]

		hydrogels			
s.no.	experiment	PCZH	PFZH	PZH	instrumental technique used
1	physical profile of beads				
	•swelling index	199.44 ± 0.02%	238.93 ± 0.02%	243.51 ± 0.02%	analytical weighing balance
	•dimensions (diameter × height)	3.6 ± 0.01 mm × 10 ± 0.01 mm	3.6 ± 0.01 mm × 10 ± 0.01 mm	4.0 ± 0.01 mm × 11 ± 0.01 mm	screw gauge
2	morphology	mesoporous surface	coarse surface with ridges	coarse mesoporous surface	scanning electron microscopy
3	porosity				
	•average pore size (nm)	0.55 ± 0.01	0.27 ± 0.01	0.68 ± 0.01	Brunauer–Emmet–Teller surface analyser
	•pore volume ($cm^3\ g^{-1}$)	$5.35 \pm 0.05 \times 10^{-4}$	$2.97 \pm 0.05 \times 10^{-4}$	$5.22 \pm 0.05 \times 10^{-4}$	
	•surface area ($m^2\ g^{-1}$)	1.95 ± 0.02	2.15 ± 0.02	1.54 ± 0.02	
4	thermal stability	major weight loss due to disruption of cross-links (41.84 ± 0.02%)	major weight loss due to disruption of cross-links (43.09 ± 0.02%)	major weight loss on polymer degradation (40.5 ± 0.02%)	thermal analyzer
		estimated metal content: 13.78 ± 0.02%	estimated metal content: 12.52 ± 0.02%	estimated metal content: 9.55 ± 0.02%	
5	crystallinity of beads				
	•crystallite size (nm)	2.30 ± 0.01	1.65 ± 0.01	1.35 ± 0.01	X-ray diffractometer
	•degree of crystallinity (%)	22.60 ± 0.02%	14.38 ± 0.02%	17.93 ± 0.02%	
6	adsorption thermodynamics				
	•standard Gibbs free energy of adsorption, ΔG^o ($kJ\ mol^{-1}$)				
	298 K	−37.13 ± 0.02	−43.07 ± 0.02	−43.48 ± 0.02	
	308 K	−40.84 ± 0.02	−46.43 ± 0.02	−48.36 ± 0.02	
	318 K	−45.08 ± 0.02	−51.85 ± 0.02	−51.76 ± 0.02	
	•standard enthalpy of adsorption, ΔH^o ($kJ\ mol^{-1}$)	−81.22 ± 0.02	−48.30 ± 0.02	−163.99 ± 0.02	ΔH^o and ΔS^o is calculated by Van't Hoff equation
	•standard entropy of adsorption, ΔS^o ($J\ mol^{-1}\ K^{-1}$)	274.99 ± 0.02	185.12 ± 0.02	572.42 ± 0.02	
7	batch fluoride adsorption studies				
	•pH	3.0 ± 0.2–9.0 ± 0.2	3.0 ± 0.2–9.0 ± 0.2	3.0 ± 0.2–9.0 ± 0.2	bench-top meter with fluoride-ion-selective electrode
	•contact time	6 ± 0.02 h–12 ± 0.02 h	6 ± 0.02 h–12 ± 0.02 h	6 ± 0.02 h–12 ± 0.02 h	
	•initial fluoride concentration	10 ± 0.2 mg L^{-1}	10 ± 0.2 mg L^{-1}	10 ± 0.2 mg L^{-1}	
	•ion interference (Cl^-,NO_3^-,HCO_3^-, PO_4^{3-} and SO_4^{2-})	negligible	negligible	negligible	
	•regenerability (% fluoride removal after the 10^{th} cycle)	97 ± 0.02	95 ± 0.02	99 ± 0.02	
	•metal leaching from the adsorbent	Cu^{2+} = 0.040 ± 0.030 mg L^{-1}	Fe^{3+} = 0.230 ± 0.020 mg L^{-1}	Zr^{4+} = 0.017 ± 0.002 mg L^{-1}	inductively coupled plasma–mass spectrometry
		Zr^{4+} = 0.017 ± 0.002 mg L^{-1}	Zr^{4+} = 0.017 ± 0.002 mg L^{-1}		

https://doi.org/10.1021/acsomega.2c00834
ACS Omega 2022, 7, 15048−15063

Table 2. Parameters of Fixed-Bed Column Studies of Hydrogel Beads Obtained from the Breakthrough Curves

beads	flow rate (±0.01 mL min^{-1})	bed height (±0.2 cm)	m_{in} (±0.02 mg)	m_{ads} (±0.02 (mg)	t_b (±0.02 h)	t_s (±0.02 h)	q_e (±0.05 mg g^{-1})	q_b (±0.05 mg g^{-1})	V_{eff} (±1 mL)	EBCT (±0.03 min)	MTZ (±0.02 cm)	% fluoride removal (±0.02%)
PCZH	0.50	2	15.60	9.38	12	47	10.43	5.73	1560	5.31	1.49	60.15
	0.10	4	6.18	4.59	46	97	2.55	1.45	618	53.10	2.10	74.34
	0.50	4	27.60	17.38	23	87	9.66	3.55	2760	11.02	2.94	62.99
	1.00	4	50.40	31.08	19	79	17.26	4.74	5040	5.31	3.03	61.66
	0.50	8	54.30	40.05	70	167	11.13	5.50	5430	21.24	4.65	73.76
PZH	0.50	2	29.77	15.53	11	74	16.84	6.57	2460	5.31	1.70	50.93
	0.10	4	15.39	7.05	26	203	3.92	0.56	1272	53.10	3.48	45.81
	0.50	4	60.98	34.02	23	162	18.90	4.80	5040	11.02	3.43	55.78
	1.00	4	102.37	57.02	21	135	31.67	1.82	8460	5.31	3.38	55.68
	0.50	8	95.83	55.41	55	255	15.39	5.23	7920	21.24	6.27	57.83
PFZH	0.50	2	14.40	7.29	8	39	8.10	4.39	1380	5.31	1.59	50.67
	0.10	4	7.38	2.81	53	115	2.54	1.64	738	53.10	2.16	61.90
	0.50	4	24.90	13.74	20	78	7.63	2.84	2490	11.02	2.97	55.20
	1.00	4	36.60	21.32	18	56	11.84	5.60	3660	5.31	2.71	58.24
	0.50	8	48.30	29.73	59	153	8.26	4.50	4830	21.24	4.92	60.92

water is 1 mg L^{-1}, as per the Bureau of Indian Standards (BIS), while it is 1.5 mg L^{-1} according to the World Health Organization (WHO). Ingestion of excess fluoride causes dental, skeletal, and non-skeletal fluorosis. Moreover, accumulation of fluoride in the body has adverse effects on the gastrointestinal, reproductive, and nervous systems.[5]

There are several mitigation strategies used to curb the fluoride menace, namely, ion exchange, precipitation, adsorption, electrocoagulation, nanofiltration, and other membrane processes.[6,7] Membrane filtration and electrocoagulation techniques are energy-intensive and have high maintenance costs. The membrane and electrodes used for the process need frequent replacement and are often costly.[8] However, adsorption has attracted wide attention of researchers due to its cost-effectiveness, high selectivity, and good efficiency. In order to establish a contact between the adsorbate and the adsorbent, different adsorption techniques are used which include batch, continuous fixed-bed, continuous moving bed, continuous fluidized bed, and pulsed-bed adsorption.[9] Though batch fluoride adsorption studies are effective in the optimization of various parameters, column fluoride adsorption studies are effective in proving the practical applicability of the adsorbents for water treatment. The adsorbent is tightly packed in a column, and the fluoride solution passes through it continuously at a fixed flow rate. This model is widely used in industries to treat a large quantity of pollutants.[9] Thus, in the current work, fixed-bed adsorption studies are carried out with the metal ion-complexed PVA hydrogel beads for efficient fluoride removal to develop potent filters for defluoridation.

Although there are many reports on batch adsorption studies for fluoride removal, there are a few reports in literature about fixed-bed column studies as the process is time-consuming and requires a longer optimization time.[9] Nevertheless, mathematical modeling of the fixed-bed column adsorption process reduces the time required for optimization of column parameters for efficient adsorption. Moreover, careful experimental design of different parameters involved in the study could be done by using a surface response methodology to make the process very efficient and to minimize the optimization time.[10,11] So far, researchers have used clays, metal-loaded bio-sorbents, mixed metal oxides, and carbonaceous materials as adsorbents for the fixed-bed fluoride adsorption studies. However, the materials reported so far have not been effective in the defluoridation of groundwater due to high interference from other competing ions.[6,7,12−17] Moreover, these adsorbents have good fluoride removal capacity predominantly at an acidic pH. To overcome these challenges, self-assembled zirconium (PZH)-, iron−zirconium (PFZH)-, and copper−zirconium (PCZH)-complexed PVA hydrogel beads are synthesized, which have good regenerability, wide pH applicability, and good selectivity for fluoride even for groundwater samples.[18] In the current study, the fluoride adsorption efficiency by the fixed-bed column of cylindrical metal−PVA hydrogel beads is explored by experimental techniques. In addition, mathematical modeling of the breakthrough curve is done to obtain the parameters for fixed-bed column adsorption. To the best of our knowledge, this is the first study on a fixed-bed column of metal−PVA hydrogel beads for effective fluoride adsorption from the groundwater sample. Moreover, due to good anion binding ability of the hydrogel beads, they are also tested for the removal of potentially toxic metal ions like

https://doi.org/10.1021/acsomega.2c00834
ACS Omega 2022, 7, 15048−15063

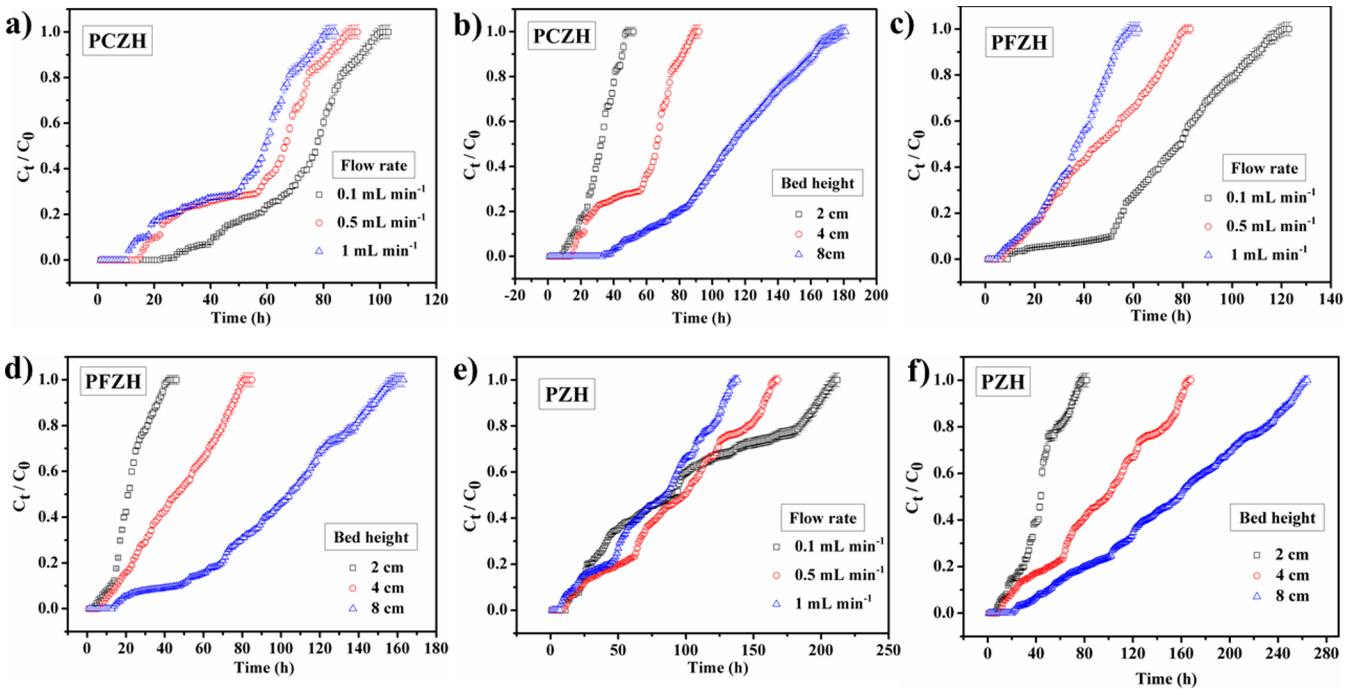

Figure 1. Breakthrough curves (C_t/C_0 vs time) for the fixed-bed fluoride adsorption by PCZH, PFZH, and PZH, variation in: (i) flow rate (a,c,e), and (ii) bed height (b,d,f).

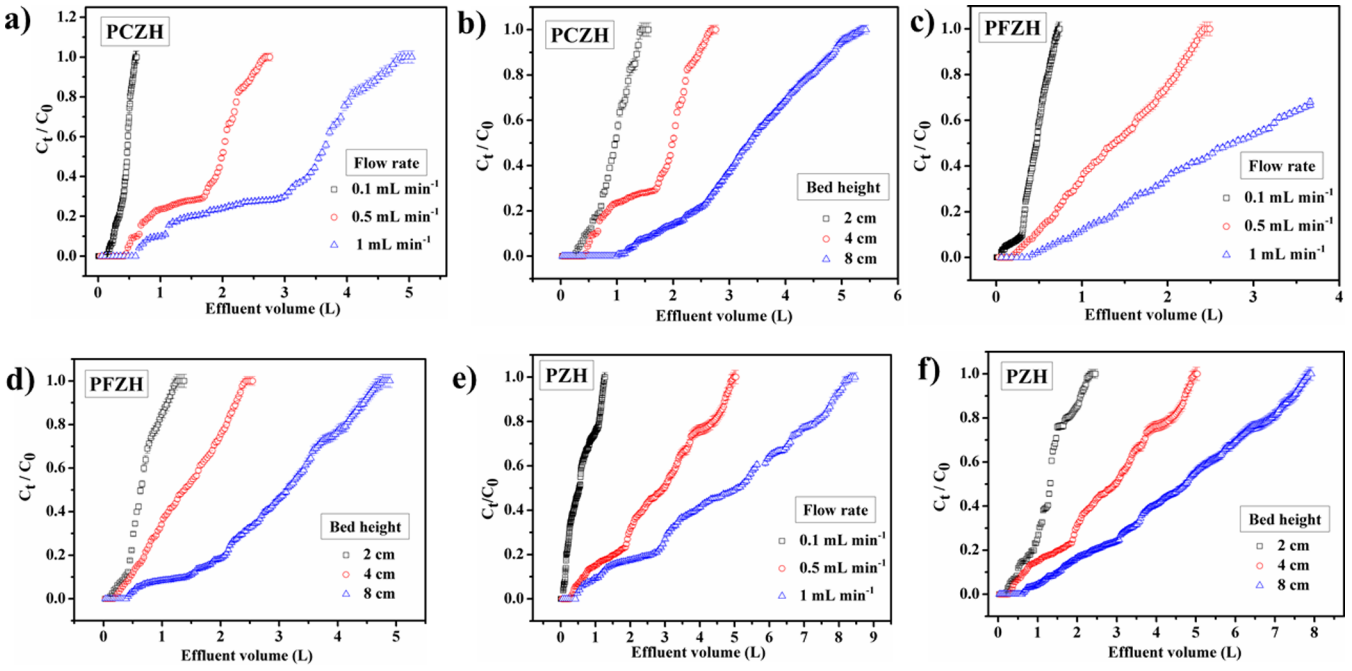

Figure 2. Breakthrough curves (C_t/C_0 vs effluent volume) for fluoride adsorption by PCZH, PFZH, and PZH, variation in: (i) flow rate (a,c,e), and (ii) bed height (b,d,f).

arsenic (V) and chromium (VI), which predominantly exist as AsO_4^{3-} and CrO_4^{2-}, respectively, in aqueous solution.[19,20] Therefore, the hydrogel beads could be used for the effective removal of fluoride, arsenate, and chromate ions.

2. MATERIALS AND METHODS

2.1. Materials. Zirconium oxychloride octahydrate ($ZrOCl_2{\cdot}8H_2O$, 98%) and *trans*-1,2 diaminocyclohexane-*N*,*N*,*N*,*N*-tetraacetic acid monohydrate (CDTA monohydrate, 98%) were purchased from Sigma-Aldrich. Polyvinyl alcohol (molecular weight = 1,45,000; degree of hydrolysis = 98−99%), sodium fluoride (NaF, 99.99%), sodium hydroxide (NaOH, 99%), hydrochloric acid (HCl, 37−38%), acetic acid (CH_3COOH, 96%), copper sulfate pentahydrate ($CuSO_4{\cdot}5H_2O$, 99%), ferric nitrate nonahydrate [$Fe(NO_3)_3{\cdot}9H_2O$, 98%], glutaraldehyde [$OHC(CH_2)_3CHO$, 50 wt % solution in H_2O], and potassium chromate (K_2CrO_4, 98.5%) were procured from Merck, India. Sodium arsenate heptahydrate ($Na_2HAsO_4{\cdot}7H_2O$, 98%) was obtained from Loba Chemie

https://doi.org/10.1021/acsomega.2c00834
ACS Omega 2022, 7, 15048−15063

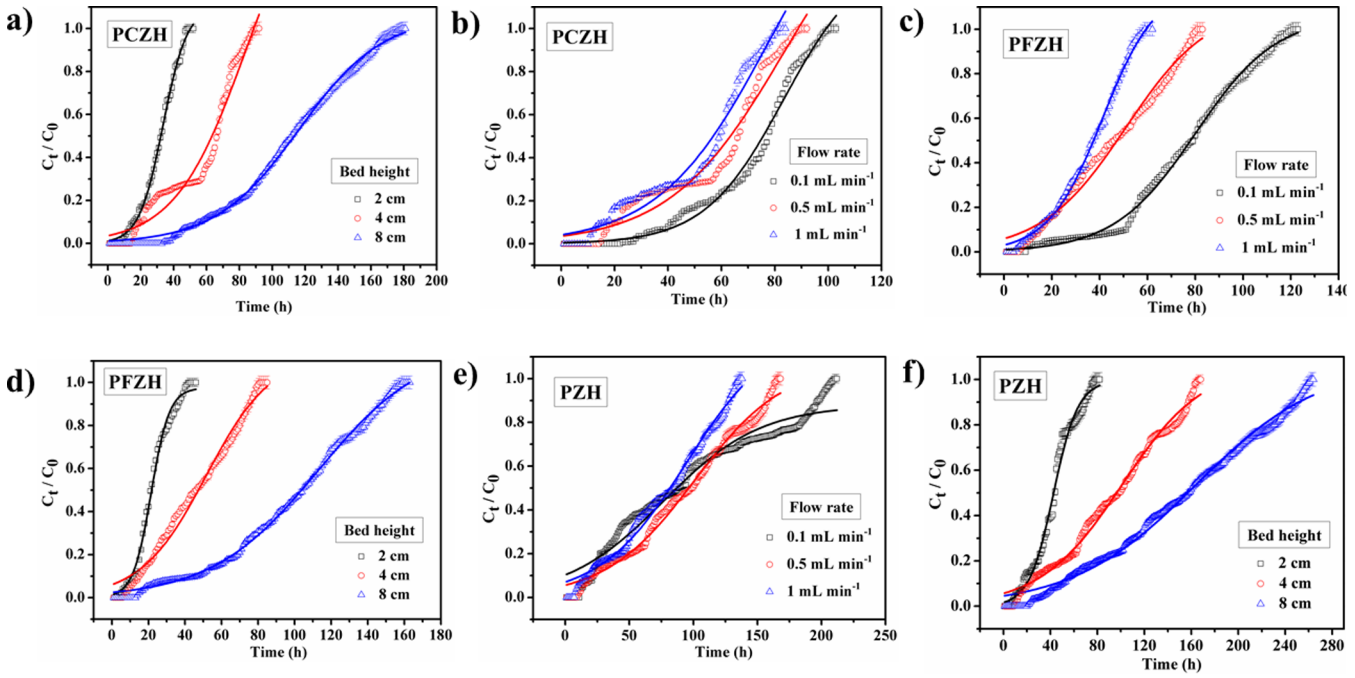

Figure 3. Non-linear mathematical model fit (Thomas, Bohart−Adams, and Yoon−Nelson) for the breakthrough curves of PCZH, PFZH, and PZH, variation in: (i) flow rate (a,c,e) and (ii) bed height (b,d,f).

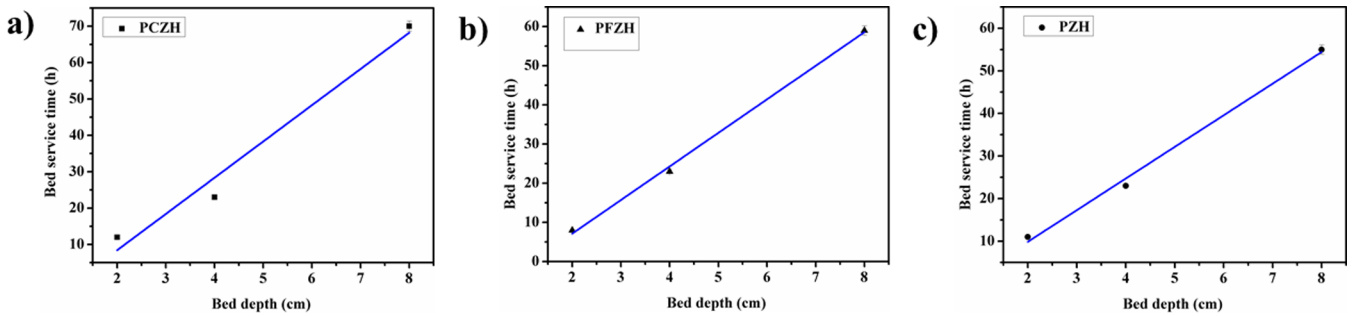

Figure 4. BDST model: (a) PCZH, (b) PFZH, and (c) PZH.

Pvt. Ltd., India. All chemicals were of analytical grade and used without further processing. The solutions were prepared in Milli-Q water (Direct Q UV-8, 18 MΩ cm^{-1}).

2.2. Synthesis of Metal-Ion−PVA Hydrogel Beads. The metal-ion−PVA hydrogel beads are obtained by simple one-pot synthesis. A 10 wt % (w/v) solution of PVA and 0.20 ± 0.02 mol L^{-1} of the metal salt with 20 ± 0.02 μL of 50 wt % (v/v) glutaraldehyde are added in a vial, and the solution is homogenized in a vortex shaker. The solution gelates and self-assembled cylindrical beads are formed on heating at 70 ± 2 °C. The hydrogel beads are washed and subjected to freeze−thaw cycles.[18] Finally, the polymer hydrogel beads are dried at 90 ± 2 °C and used for column adsorption studies.

2.3. Optimization of Column Parameters. The physico-chemical characterization of the metal-ion-incorporated hydrogel beads is performed. The effects of pH, temperature, interfering ions, and initial fluoride concentrations on the batch adsorption process are optimized (Table 1). The experimental results of fluoride adsorption studies and the characterization of the hydrogel beads establish that fluoride uptake occurs mainly by chemical bonding, hydrogen bonding, and pore diffusion. The thermodynamic parameters of adsorption are computed from the adsorption equilibrium studies at 25, 35, and 45 °C.[21,22] The standard Gibb's free energy of adsorption (ΔG^{o}) is calculated as

$$\Delta G^{o} = -RT \ln K_{c} \quad (1)$$

where K_C, the dimensionless equilibrium constant, is obtained by converting Langmuir constant K_L, which is given by eq 2.

$$K_{C} = 55.5 \times 1000 \times K_{L} \times M_{w} \quad (2)$$

where M_w is the molar mass of the analyte used in the study (i.e., NaF).

The standard enthalpy (ΔH^{o}) and standard entropy (ΔS^{o}) of adsorption are obtained from the van't Hoff equation

$$\ln K_{C} = \frac{-\Delta H^{o}}{R} \times \frac{1}{T} + \frac{\Delta S^{o}}{R} \quad (3)$$

The evidence of chemisorption of fluoride by the hydrogel beads is confirmed by thermodynamic calculations of batch adsorption studies (Table 1).[18] This is also reinforced by the Fourier transform infrared (FT-IR) spectral analysis of the hydrogel beads. The spectra of hydrogel beads are obtained using a FT-IR spectrophotometer (Spectrum 2, PerkinElmer,

https://doi.org/10.1021/acsomega.2c00834
ACS Omega 2022, 7, 15048−15063

Table 3. Mathematical Modeling of the Breakthrough Curves

			Bohart–Adams		Thomas		Yoon–Nelson		
beads	bed height (±0.2 cm)	flow rate (±0.0003 L h^{-1})	k_{BA} (±0.05 L mg^{-1} h^{-1})	N_0 (±0.05 mg L^{-1})	k_{Th} (±0.0001 L mg^{-1} h^{-1})	q_0 (±0.05 mg g^{-1})	k_{YN} (±0.05 h^{-1})	τ (±0.05 h)	R^2
PCZH	2	0.030	1.36×10^{-2}	91.52	1.36×10^{-2}	11.20	1.36×10^{-1}	33.61	0.99
	4	0.006	6.79×10^{-3}	76.38	6.79×10^{-3}	2.77	6.79×10^{-2}	83.20	0.99
	4	0.030	4.84×10^{-3}	361.03	4.84×10^{-3}	13.11	4.84×10^{-2}	78.66	0.96
	4	0.060	4.85×10^{-3}	706.65	4.85×10^{-3}	25.66	4.85×10^{-2}	76.98	0.97
	8	0.030	3.92×10^{-3}	133.47	3.92×10^{-3}	9.69	3.92×10^{-2}	116.28	0.99
PZH	2	0.030	9.58×10^{-3}	116.15	9.58×10^{-3}	14.22	9.58×10^{-2}	42.65	0.99
	4	0.006	2.18×10^{-3}	85.13	2.18×10^{-3}	3.09	2.18×10^{-2}	76.64	0.96
	4	0.030	2.37×10^{-3}	561.63	2.37×10^{-3}	20.39	2.37×10^{-2}	101.12	0.99
	4	0.060	2.45×10^{-3}	1049.23	2.45×10^{-3}	38.17	2.96×10^{-2}	94.63	0.99
	8	0.030	1.57×10^{-3}	227.63	1.57×10^{-3}	16.53	1.57×10^{-2}	163.90	0.99
PFZH	2	0.030	2.01×10^{-2}	58.55	2.01×10^{-2}	7.17	2.013×10^{-1}	21.50	0.99
	4	0.006	5.88×10^{-3}	73.48	5.88×10^{-3}	2.67	5.88×10^{-2}	80.04	0.99
	4	0.030	5.66×10^{-3}	234.03	5.66×10^{-3}	8.50	5.66×10^{-2}	50.99	0.99
	4	0.060	8.88×10^{-3}	378.74	8.88×10^{-3}	13.75	8.88×10^{-3}	41.26	0.99
	8	0.030	3.43×10^{-3}	129.34	3.43×10^{-3}	9.39	3.43×10^{-2}	112.68	0.99

Table 4. Parameters Obtained from the BDST Model for the Hydrogel Beads

beads	N_0 (±0.05 mg L^{-1})	k_{BDST} (±0.0001 L mg^{-1} min^{-1})	R^2
PCZH	67.04	1.51×10^{-2}	0.95
PFZH	57.67	1.74×10^{-2}	0.99
PZH	60.47	3.47×10^{-2}	0.99

USA). Furthermore, for the fixed-bed column adsorption studies, parameters such as bed height and flow rate are optimized.

2.3.1. Lab-Scale Fixed-Bed Column Adsorption Studies. Fabricated borosilicate glass columns with 1.3 cm inner and 1.5 cm outer diameters and lengths of 5 and 10 cm are used for the study. These dimensions are chosen to make a potent portable fluoride water filter for commercial applicability.[23] The dried hydrogel beads are packed into the column and plugged with cotton on either side of inlet and outlet, for continuous flow fixed-bed studies. Columns with bed heights of 2 ± 0.2, 4 ± 0.2, and 8 ± 0.2 cm are chosen for the study. On passing the fluoride solution, the hydrogels swell up due to the high swelling ability, thereby reducing the void spaces in the column. As the hydrogels exhibit pH-independent behavior in a wide pH range (3.0 ± 0.2−9.0 ± 0.2), the column adsorption is carried out with a fluoride solution of pH 6.5 ± 0.2 (Table 1).[18] The groundwater fluoride concentration is generally found to be ≤10 ± 0.20 mg L^{-1} in India.[1,2,4] Hence, for fixed-bed column adsorption, the influent fluoride concentration (C_0) is maintained at 10 ± 0.20 mg L^{-1}, and all the studies are conducted at 25 °C. Three different flow rates (0.10 ± 0.01, 0.50 ± 0.01, and 1.0 ± 0.01 mL min^{-1}) are maintained using a peristaltic pump (Ismatec Reglo ICC, Cole Parmer, Germany) with the fluoride influent pumped in the upward direction to avoid channeling.[17] The adsorbent bed heights are fixed at 2 ± 0.02 cm (adsorbent dosage = 0.9 g), 4 ± 0.02 cm (adsorbent dosage = 1.8 g), and 8 ± 0.02 cm (adsorbent dosage = 3.6 g). Water is collected from the column outlet every hour, and the effluent fluoride concentration (C_t) is measured using a bench top meter with a fluoride-ion selective electrode (Orion A124, Thermo Fischer Scientific, USA) using TISAB II.[24] The fluoride ion-selective electrode has a limit of detection of ±0.02 mg L^{-1} (10^{-6} mol L^{-1}) and could be used in the temperature range of 0−80 °C. The reproducibility of data is ±2% on regular calibration, and the electrode has a linear range of operation for a slope between −54 and −60 mV. This is obtained by calibrating the electrode with three fluoride standards of a 10-fold difference in the concentration. The electrode could be used for the detection of the fluoride concentration as low as 0.02 mg L^{-1}.

2.4. Evaluation of the Breakthrough Curve. The performance of the column packed with PZH, PCZH, and PFZH beads are evaluated based on the breakthrough curves. Breakthrough curves are a plot of the ratio of effluent concentration to the influent concentration (C_t/C_0) versus time. The shape of the breakthrough curve and time required for breakthrough plays a significant role in interpreting the dynamic behavior of the column and improves the operational design. The steepness of the breakthrough curve also provides the information about the extent to which the adsorbent bed could be utilised.[25]

The column breakthrough time (t_b) is taken when C_t ≤1.5 ± 0.2 mg L^{-1} and the saturation time (t_s) is chosen when the

https://doi.org/10.1021/acsomega.2c00834
ACS Omega 2022, 7, 15048−15063

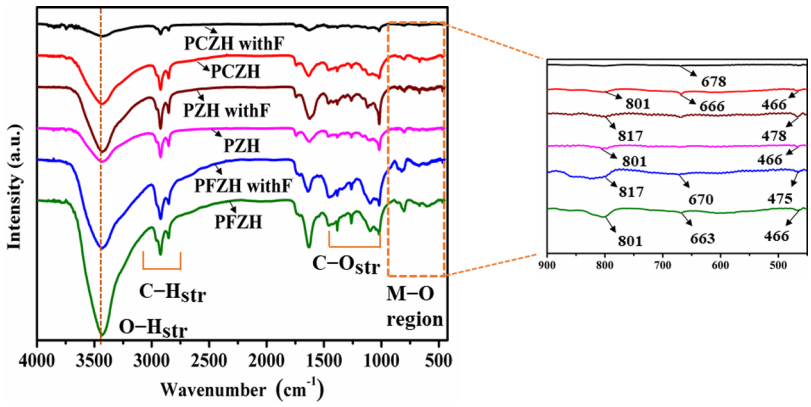

Figure 5. FT-IR spectra of polymer hydrogel beads before and after fluoride adsorption.

Scheme 1. Mechanism of Fluoride Adsorption by Fixed-Bed Column of Metal–PVA Hydrogel Beads

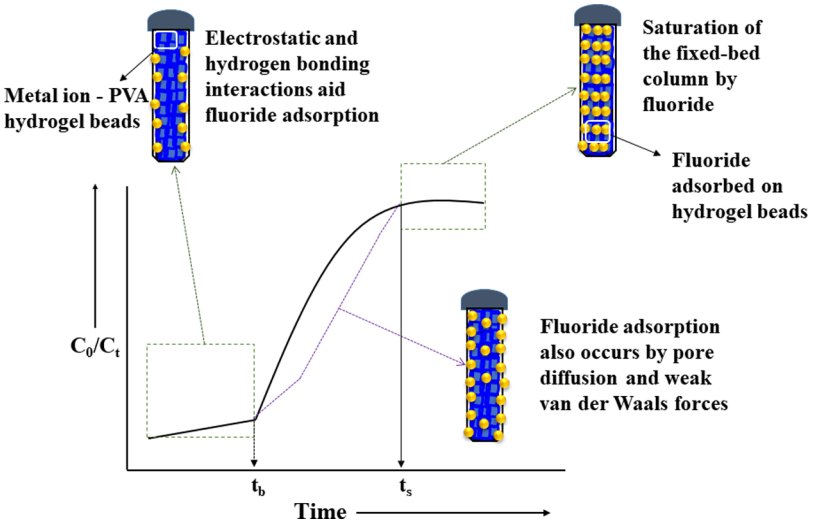

Table 5. Evaluation of the Column Performance

beads	flow rate (±0.01 mL min^{-1})	bed height (±0.2 cm)	DoSU (±0.02%)	SUR (±0.05 g L^{-1})	number of bed volumes (±0.10)
PCZH	0.50	2	54.94	12.50	135.68
	0.10	4	56.93	6.52	52.01
	0.50	4	37.42	2.61	138.03
	1.00	4	28.03	1.58	214.83
	0.50	8	59.30	0.85	197.87
PZH	0.50	2	52.14	13.64	124.37
	0.10	4	22.07	11.53	29.40
	0.50	4	25.68	2.61	130.03
	1.00	4	5.82	1.43	237.44
	0.50	8	34.20	2.18	155.47
PFZH	0.50	2	61.71	18.75	90.45
	0.10	4	65.42	5.66	59.93
	0.50	4	38.05	3.00	113.07
	1.00	4	51.67	1.67	203.52
	0.50	8	55.09	2.03	166.77

effluent concentration is 95% of the initial concentration (10 ± 0.2 mg L^{-1}).[14,26] The effluent volume (V_{eff}) passing through the column is given by

$$V_{eff} = Q\ t_e \quad (4)$$

where Q is the flow rate (L h^{-1}) and t_e is the column exhaustion time.[27]

The amount of fluoride in the column ($m_{in,t}$, mg) at time, t (h), is given by

$$m_{in,t} = C_0 Q\ t \quad (5)$$

where Q is the flow rate (L h^{-1}) and C_0 is the initial concentration of the fluoride solution (mg L^{-1}).

https://doi.org/10.1021/acsomega.2c00834
ACS Omega 2022, 7, 15048−15063

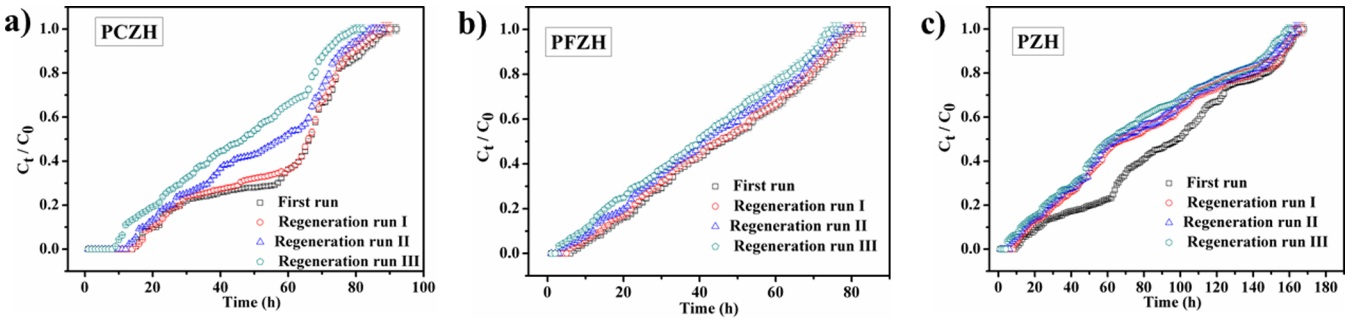

Figure 6. Regeneration curves for the fixed-bed column adsorption: (a) PCZH, (b) PFZH, and (c) PZH.

The amount of unadsorbed fluoride ($m_{out,t}$, mg) at time, t, is calculated by multiplying the area under the dimensionless curve with the initial concentration, C_0, and the flow rate (Q) is given by the equation

$$m_{out,t} = C_0 Q \int_0^t \left(\frac{C_t}{C_0}\right) dt \tag{6}$$

The amount of fluoride adsorbed ($m_{ad,t}$, mg) by the column is given by

$$m_{ads,t} = m_{in,t} - m_{out,t} \tag{7}$$

The equilibrium uptake capacity (q_e, mg g^{-1}) by the column at saturation time (t_s) is given by the equation

$$q_e = \frac{m_{ads,t_s}}{M} = \frac{C_0 Q \int_0^{t_s} \left(1 - \frac{C_t}{C_0}\right) dt}{M} \tag{8}$$

The uptake at breakthrough is given by

$$q_b = \frac{m_{ads,t_b}}{M} = \frac{C_0 Q \int_0^{t_b} \left(1 - \frac{C_t}{C_0}\right) dt}{M} \tag{9}$$

where M is the mass of the adsorbent in grams.[23]

The fluoride adsorption efficiency of the column packed with hydrogel beads is given by

$$\%\ \text{Fluoride removal} = \frac{m_{ads,\,t}}{m_{in,\,t}} \times 100 \tag{10}$$

The empty bed contact time (EBCT) of the column is defined as

$$\text{EBCT} = \frac{\text{Bed volume(mL)}}{\text{Flow rate(mL min}^{-1})} \tag{11}$$

The greater values of removal efficiency, breakthrough time, and saturation time indicate the good adsorption ability of the hydrogel beads packed in the column.

3. RESULTS AND DISCUSSION

The efficiency of fluoride removal is largely dependent on the bed height of the column and the flow rate of the analyte.[9] The nature of the breakthrough curve is understood by predicting the mass-transfer zone (MTZ) that exists in a fixed-bed column. This is given by the equation

$$\text{MTZ} = \left(1 - \frac{t_b}{t_s}\right) \times L \tag{12}$$

where L is the length of the column, t_b is the breakthrough time, and t_s is the saturation time.

As a fluoride solution passes through the adsorbent in the column, in the upward direction, the adsorbent in the lower layers of the column adsorbs rapidly ($C_t/C_0 = 0$). With time, the lower layers get saturated and adsorption occurs in the unadsorbed layers of the adsorbent and eventually, the column gets saturated ($C_t/C_0 = 1$). Thus, at a particular initial concentration of the analyte, the rate at which the column saturates depends on the flow rate (Table 2). Moreover, the time required for column saturation also escalates on increasing the bed height (Table 2). The breakthrough curves are plotted with respect to time and treated effluent volume (Figures 1 and 2).

3.1. Effect of the Flow Rate on Fluoride Adsorption by Metal−PVA Hydrogel Beads. The fixed-bed fluoride adsorption by the hydrogel beads is studied at three different flow rates with a constant bed height of 4 ± 0.2 cm and an inlet fluoride concentration of 10 ± 0.2 mg L^{-1}. It is observed that on increasing the flow rate from 0.10 ± 0.01 to 1 ± 0.01 mL min^{-1}, the breakthrough and saturation time decrease.[28] This is because the contact time of fluoride with the adsorbent decreases on increasing the flow rate (Table 2). Moreover, the fluoride removal efficiency is better for the hydrogel beads at a lower flow rate as fluoride gets sufficient time for interaction with the hydrogel beads. This also justifies the higher breakthrough time for PCZH, PZH, and PFZH at 46 ± 0.02, 26 ± 0.02, and 53 ± 0.02 h, at a flow rate of 0.10 ± 0.01 mL min^{-1} (Figure 1a,c,e). However, on increasing the flow rate, the equilibrium fluoride adsorption capacity and the treated effluent volume increases. This is because at a flow rate of 1 ± 0.01 mL min^{-1}, more amount of fluoride passes through the column (m_{int}) and the fluoride adsorbed (m_{ads}) by the column increases (Table 2).[25] The fluoride removal capacities are 31.67 ± 0.05 mg g^{-1} (PZH), 17.26 ± 0.05 mg g^{-1} (PCZH), and 11.84 ± 0.05 mg g^{-1} (PFZH) for an effluent flow rate of 1 ± 0.01 mL min^{-1}. Hence, a greater volume of fluoridated water is treated at a higher flow rate (Figure 2). However, to facilitate sufficient adsorbent contact time with fluoride and to improve the fluoride removal efficiency, the flow rate of the analyte is fixed at 0.50 ± 0.01 mL min^{-1}.

3.2. Effect of Bed Height on Fluoride Adsorption by Metal−PVA Hydrogel Beads. The adsorbent bed height also plays a crucial role in designing the column for groundwater treatment. Raising the height of packed adsorbent in the column from 2 ± 0.2 to 8 ± 0.2 cm at 0.50 ± 0.01 mL min^{-1} flow rate brings about an increase in the column breakthrough time (t_b), saturation time (t_s),

https://doi.org/10.1021/acsomega.2c00834
ACS Omega 2022, 7, 15048−15063

Table 6. Regeneration of Hydrogel Beads Post-Fluoride Adsorption

	0th cycle			1st cycle			regeneration cycle			2nd cycle			3rd cycle		
beads	% fluoride removal (±0.02%)	q_e (±0.05 mg g^{-1})	V_{eff} (±1 mL)	% fluoride removal (±0.02%)	q_e (±0.05 mg g^{-1})	V_{eff} (±1 mL)	% fluoride removal (±0.02%)	q_e (±0.05 mg g^{-1})	V_{eff} (±1 mL)	% fluoride removal (±0.02%)	q_e (±0.05 mg g^{-1})	V_{eff} (±1 mL)	% fluoride removal (±0.02%)	q_e (±0.05 mg g^{-1})	V_{eff} (±1 mL)
PCZH	62.98	9.67	2700	62.89	9.43	2690	58.08	8.52	2640	54.18	7.40	2460			
PZH	57.83	18.90	5040	48.03	16.17	5010	46.93	15.61	4950	45.74	14.85	4830			
PFZH	55.20	7.63	2490	54.52	7.45	2460	52.33	6.98	2400	50.91	6.53	2310			

treated effluent volume (V_{eff}), and MTZ (Table 2). Hence, the column efficiency depends on the adsorbent bed height. It is observed that the effective MTZ increases on raising the bed height in the fixed-bed column.[29] The EBCT increases as the bed height is increased. EBCT of the column with bed heights, 2 ± 0.2, 4 ± 0.2 and 8 ± 0.2 cm are 5.31 ± 0.03, 10.62 ± 0.03 and 21.24 ±0.03 min, respectively. It is observed that the fluoride removal efficiency of the column is higher for 8 ± 0.2 cm bed height as the adsorbate−adsorbent interaction is prolonged due to high EBCT (Table 2).[30] Not only that, the column saturation time nearly triples for PCZH (47 ± 0.02 to 167 ± 0.02 h), PZH (74 ± 0.02 to 255 ± 0.02 h), and PFZH (39 ± 0.02 to 153 ± 0.02 h) when the bed height changes from 2 ± 0.2 to 8 ± 0.2 cm. This substantiates that the column with a greater bed height could be used for a longer period of time (Figure 1b,d,f). Moreover, a larger effluent volume is treated and the efficiency of the column also improves at a bed height of 8 ± 0.2 cm (Figure 2b,d,f).

3.3. Column Adsorption Models. The breakthrough curves are analyzed using the three empirical kinetic models, namely, Thomas, Bohart−Adams, Yoon−Nelson, and a semi-empirical bed depth service time (BDST) model, to obtain different parameters for fixed-bed adsorption[31] (Figures 3 and 4). These models are chosen specifically to obtain the maximum adsorption capacity and half-time of breakthrough of the column, to understand the mechanism of adsorption and efficacy of the column for fluoride removal.[25] The empirical models can be mathematically simplified into the following non-linear expression[23,31] which is given by

$$\frac{C_t}{C_0} = \frac{1}{1 + e^{(a-bt)}} \tag{13}$$

However, the parameters "*a*" and "*b*" are different in the models.

3.3.1. Thomas Model. The Thomas model is based on the assumption that equilibrium adsorption data follows the Langmuir adsorption isotherm and obeys pseudo-second-order kinetics.[27] The model assumes that the rate-limiting step is devoid of diffusion and axial dispersion.

The linear equation of the Thomas model is given by

$$\ln\left(\frac{C_0}{C_t} - 1\right) = \frac{k_{Th} q_0 m}{Q} - k_{TH} C_0 t \tag{14}$$

where k_{Th} is the Thomas rate constant (L mg^{-1} h^{-1}), C_0 is the initial fluoride concentration (mg L^{-1}), C_t is the fluoride concentration at any time, t (mg L^{-1}), q_0 is the fluoride adsorbed per unit gram of the adsorbent (mg g^{-1}), m is the mass of the adsorbent (g), and Q is the flow rate of the adsorbent (L h^{-1}).

The non-linear equation of the Thomas model can be expressed in the form of eq 13, which is given as

$$\frac{C_t}{C_0} = \frac{1}{1 + e^{\left(\frac{k_{Th} q_0 m}{Q} - k_{Th} C_0 t\right)}} \tag{15}$$

The data obtained from the fixed-bed column studies are fitted in the Thomas model (Figure 3). Parameter k_{Th} decreases with the increase in the flow rate (Table 3). This indicates that a fluoride uptake predominantly occurs by chemisorption. Moreover, the equilibrium adsorption data for hydrogel beads fit well in the Langmuir adsorption isotherm

https://doi.org/10.1021/acsomega.2c00834
ACS Omega 2022, 7, 15048−15063

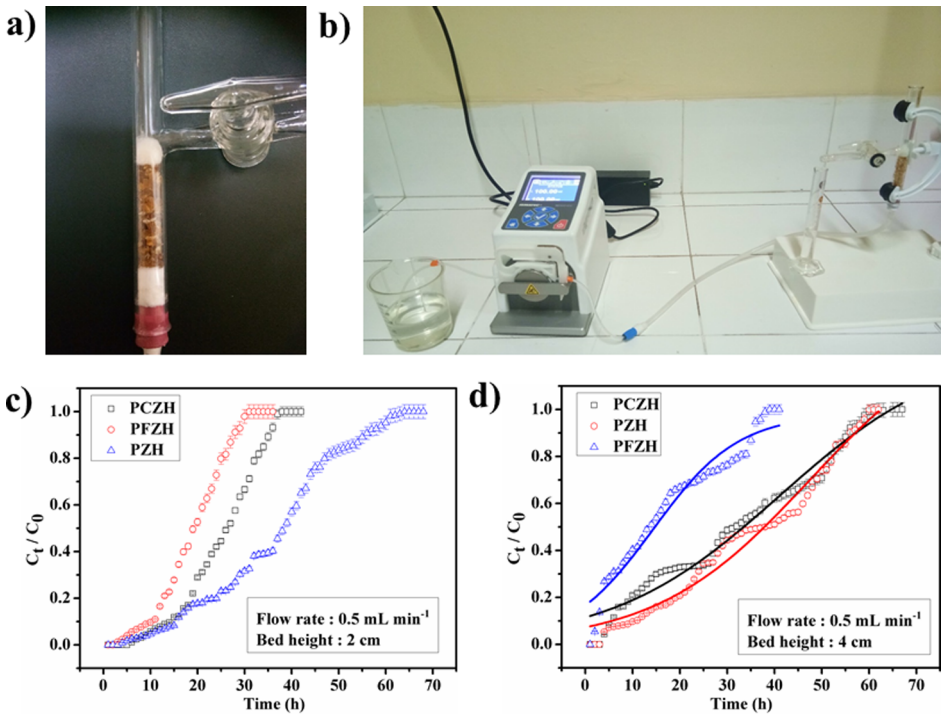

Figure 7. (a) Borosilicate-column packed with PFZH beads, (b) laboratory-scale column set up, (c) ion-interference studies, and (d) non-linear model fit (Thomas, Bohart–Adams, and Yoon–Nelson) for breakthrough curves of groundwater sample.

Table 7. Physico-Chemical Analysis of Groundwater Before and After Fluoride Adsorption

		after adsorption		
parameter	before adsorption	PCZH	PFZH	PZH
pH (±0.01)	8.12	7.10	7.20	6.72
TDS (±2 mg L^{-1})	1100	245	257	290
hardness (±0.01 mg L^{-1})	856.00	821.76	770.40	719.04
Na^+ (±0.01 mg L^{-1})	308.10	299.70	304.81	288.80
K^+ (±0.01 mg L^{-1})	3.38	3.26	3.35	3.11
Mg^{2+} (±0.01 mg L^{-1})	618.60	540.30	575.20	402.70
Ca^{2+} (±0.01 mg L^{-1})	856.65	721.65	590.05	714.89
conductivity (±0.001 mS cm^{-1})	0.070	0.063	0.061	0.061
fluoride (±0.01 mg L^{-1})	2.84	0.00	0.00	0.00

in the batch adsorption studies.[18] The value of q_0 obtained from the Thomas model is in good agreement with the calculated equilibrium capacity, q_e, indicating that this model best describes the dynamic behavior of the column.[26]

3.3.2. Bohart–Adams Model. This model is based on the assumption that equilibrium does not occur instantaneously. The rate of adsorption is proportional to residual capacity of the adsorbent and concentration of the adsorbate.[27] The linear equation of the Bohart–Adams model is given as follows

$$\ln\left(\frac{C_0}{C_t} - 1\right) = \frac{k_{BA} N_0 L}{u} - k_{BA} C_0 t \quad (16)$$

The non-linear equation for the Bohart–Adams model is given by

$$\frac{C_t}{C_0} = \frac{1}{1 + e^{\left(\frac{k_{BA} Z N_0}{F} - k_{BA} C_0 t\right)}} \quad (17)$$

where k_{BA} is the Bohart–Adams rate constant (L mg^{-1} h^{-1}), N_0 is the saturation concentration (mg L^{-1}), Z is bed depth of the column (cm), and F is the linear velocity (cm min^{-1}).

The fixed-bed column data are fitted in the Bohart–Adams model. It is observed that at a higher flow rate, the value of N_0 increases while k_{BA} decreases (Table 3). However, the value of N_0 decreases on raising the bed height, which implies that external mass transfer in the column adsorption process plays a role and the adsorption occurs slowly.[27]

3.3.3. Yoon–Nelson Model. The Yoon–Nelson model is based on the assumption that the decrease in the adsorption rate depends on the probability of adsorption of the

Table 8. Parameters of Fixed-Bed Column Studies for Fluoride Adsorption by Hydrogel Beads Obtained from Breakthrough Curves in the Presence of Interfering Ions

beads	flow rate (±0.01 mL min^{-1})	bed height (±0.2 cm)	m_{in} (±0.02 mg)	m_{ads} (±0.02 mg)	t_b (±0.02 h)	t_s (±0.02 h)	q_e (±0.05 mg g^{-1})	q_b (±0.05 mg g^{-1})	V_{eff} (±1 mL)	EBCT (±0.03 min)	MTZ (±0.02 cm)	DoSU (±0.02%)	SUR (±0.05 g L^{-1})	% fluoride removal (±0.02%)
PCZH	0.50	2	12.60	7.24	10	36	8.05	5.06	1260	5.31	1.44	62.88	3.00	57.46
PZH	0.50	2	24.68	12.75	11	60	14.17	6.15	2040	5.31	1.63	52.55	2.72	51.64
PFZH	0.50	2	10.80	5.38	6	30	5.98	3.45	1080	5.31	1.60	57.67	5.00	49.83

https://doi.org/10.1021/acsomega.2c00834
ACS Omega 2022, 7, 15048−15063

Table 9. Parameters of the Fixed-Bed Column of Hydrogel Beads for Fluoride Adsorption Obtained from Breakthrough Curves for Groundwater Sample

beads	flow rate (±0.01 mL min^{-1})	bed height (±0.2 cm)	m_{in} (±0.02 mg)	m_{ads} (±0.02 mg)	t_b (h)	t_s (h)	q_e (±0.05 mg g^{-1})	q_b (±0.05 mg g^{-1})	V_{eff} (±1 mL)	EBCT (±0.03 min)	MTZ (±0.02 cm)	DoSU (±0.02%)	SUR (±0.05 g L^{-1})	% fluoride removal (±0.02%)
PCZH	0.50	4	5.70	2.71	34	57	1.50	1.12	2010	10.62	1.61	76.67	1.76	47.44
PZH	0.50	4	5.28	3.01	41	58	1.67	1.39	1860	10.62	3.72	85.74	1.46	56.92
PFZH	0.50	4	3.49	1.39	15	36	0.77	0.44	1230	10.62	2.33	61.23	4.00	40.10

adsorbate and the occurrence of breakthrough at the adsorbent, which is given by the linear equation

$$\ln\left(\frac{C_0}{C_t} - 1\right) = k_{YN}\,\tau - k_{YN}\,t \tag{18}$$

The Yoon−Nelson model could be written in a non-linear mathematical form given by

$$\frac{C_t}{C_0} = \frac{1}{1 + e^{(k_{YN}\,\tau - k_{YN}\,t)}} \tag{19}$$

where k_{YN} is the Yoon−Nelson rate constant coefficient and τ is the time required for 50% breakthrough.[14]

On fitting the data in the Yoon−Nelson model, it is observed that the value of τ reduces at a higher flow rate (Table 3). This is because the breakthrough is attained faster due to reduction in the EBCT.[23] It is observed that k_{YN} is inversely related to the bed height.[14] The column with a greater bed height has a longer saturation time as indicated by a higher value of τ for PCZH (τ = 116 ± 0.02 h), PZH (τ = 164 ± 0.02 h), and PFZH (τ = 113 ± 0.02 h) (Table 3).

3.3.4. Bed Depth Service Time Model. The efficiency of the column depends on its ability to provide clean water for a longer duration. The service time of the column for a specific bed height is determined using the BDST model (Figure 4). The model assumes that the rate of adsorption depends on the interaction between the adsorbate and the unused adsorbent in the column bed.[9] This model was initially proposed by Bohart and Adams and later modified by Hutchins.[31] The model is based on the linear relationship between the bed height and service time of the column. This is based on the assumption that the adsorbate is directly adsorbed onto the adsorbent and there is a negligible contribution by intraparticle diffusion or mass transfer. The BDST model is given by the equation

$$t = \frac{N_0}{C_0 F} Z - \frac{1}{k_{BDST} C_0} \ln\left(\frac{C_0}{C_t} - 1\right) \tag{20}$$

where t is the time at which breakthrough is attained (min), F is the linear flow velocity (cm min^{-1}), N_0 is the adsorption capacity of the bed in mg L^{-1}, Z is the bed depth (cm), and k_{BDST} is the rate constant (L mg^{-1} min^{-1}).

The bed saturation capacity obtained from the BDST model indicates that PCZH removes a greater amount of fluoride compared to other hydrogel beads (Table 4).

3.4. Mechanism of Fluoride Adsorption. Adsorption equilibrium of the adsorbate in aqueous medium and the solid adsorbent in a fixed-bed column is generally attained due to axial dispersion, intra-particle diffusion resistance (pore and surface diffusion) and film resistance.[9] This can be explained by considering the following stages of adsorption: (1) fluoride is transported from the bulk solution into an immobile layer of ions surrounding the hydrogel beads by advective transport or axial dispersion to the hydrogel beads, (2) fluoride can penetrate through the immobile layer to reach the adsorbent surface sites, (3) adsorption can occur by the binding of fluoride to the specific sites of the adsorbent, and (4) the fluoride can also diffuse into the pores of the hydrogel beads by intraparticle diffusion. The rate of fluoride removal by hydrogel beads is dependent on one or more of these commonly reported phenomena.[32] In batch adsorption studies, stage 1 and stage 2 can be neglected as the adsorbent is stirred vigorously. However, in the fixed-bed column adsorption studies, stage 1 and 2 also play a role in the rate-determining step especially for the column of a greater bed height.[32] The binding of fluoride to the metal-incorporated PVA hydrogel beads may occur by electrostatic interaction, hydrogen bonding, and pore diffusion.[18] FT-IR analysis of spectra of the metal-incorporated hydrogel beads, post-fluoride adsorption, proves the existence of the interaction between fluoride and hydrogels (Figure 5). In the FT-IR spectrum of metal−PVA hydrogel beads, characteristic peaks of PVA such as the O−H, C−H, C=O, and C−O are present.[33] The peak corresponding to the O−H$_{str}$ is observed at 3429 cm^{-1} in the FT-IR spectra. This can be attributed to the M−OH and the free −OH groups present in the polyvinyl alcohol of the hydrogel beads.[34] The slight broadening of the O−H$_{str}$ peaks could be due to the hydrogen-bonded interaction existing between PVA chains.[35−37] The peak at 1630 cm^{-1} corresponds to the stretching of the C=C groups formed due to the heat treatment of the hydrogel beads during the synthesis.[38] The semi-crystalline nature of PVA in the hydrogel beads is confirmed by the appearance of a peak around 1100 cm^{-1} due to C−O$_{str}$ in the metal−PVA hydrogel beads. The presence of the acetal group is confirmed by the appearance of a peak at 1020 cm^{-1}, which is due to the cross-linking of PVA with glutaraldehyde.[39] Apart from this, the characteristic peaks in the region 450−850 cm^{-1} are attributed to the existence of M−O bonds.[40,41] The peaks at 801 and 466 cm^{-1} are due to the presence of Zr−O bonds in PZH, PFZH, and PCZH beads.[42] The peak for Fe−O in PFZH beads appears at 663 cm^{-1}, whereas the peak at 666 cm^{-1} is due to the Cu−O bond in PCZH beads.[41,43,44] After fluoride adsorption, the peaks in the FT-IR spectra of the hydrogel beads shift to a higher frequency with reduced intensity, indicating the interaction of fluoride with the metal ions.[45] The Zr−O peaks in the spectrum of PZH beads shift to 817 and 478 cm^{-1}. After fluoride adsorption, the Zr−O peaks in PFZH shift to 817 and 478 cm^{-1}. The Fe−O peak is shifted to 670 cm^{-1} in the spectrum of PFZH. A peak appears at 678 cm^{-1} in the spectrum for PCZH beads post-fluoride adsorption. These changes can be taken as the evidence of fluoride binding to the metal ions because the M−F

https://doi.org/10.1021/acsomega.2c00834
ACS Omega 2022, 7, 15048−15063

Table 10. Mathematical Modeling of the Breakthrough Curves of Fluoride Adsorption by Hydrogel Beads in the Groundwater Sample

			Bohart–Adams		Thomas		Yoon–Nelson		
beads	bed height (±0.2 cm)	flow rate (±0.0003 L h^{-1})	k_{BA} (±0.0001 L mg^{-1} h^{-1})	N_0 (±0.05 mg L^{-1})	k_{Th} (±0.0001 L mg^{-1} h^{-1})	q_0 (±0.05 mg g^{-1})	k_{YN} (±0.05 h^{-1})	τ (±0.02 h)	R^2
PCZH	4	0.030	1.97×10^{-2}	53.60	1.97×10^{-2}	1.95	5.60×10^{-2}	41.12	0.98
PZH	4	0.030	2.16×10^{-2}	61.87	2.16×10^{-2}	2.25	6.13×10^{-2}	47.46	0.98
PFZH	4	0.030	3.91×10^{-3}	18.70	3.91×10^{-3}	0.68	1.11×10^{-1}	14.35	0.95

absorptions generally occurring in far IR regions are undetectable by the FT-IR spectrophotometer.[45]

Moreover, the pore volume for the hydrogel beads is comparatively smaller indicating that intraparticle diffusion does not play a predominant role in enhancing the fluoride removal capacity. Besides, the breakthrough curve shows a steep increase, initially. This indicates that fluoride adsorption before the breakthrough occurs rapidly due to the availability of greater adsorbent sites (Scheme 1). Eventually, as the fluoride gets adsorbed in the lower layers of the column, the rate of adsorption slows down due to a decrease in the availability of the binding sites (Scheme 1). After the breakthrough, the fluoride adsorption might occur by physisorption and pore diffusion. The adsorption of fluoride at this stage may be controlled mainly by the mass-transfer process involving the movement of fluoride ions into these pores.[46] Therefore, the overall rate of fluoride adsorption slows down as confirmed by the low value of the rate constant obtained by fitting the breakthrough curves in the column adsorption models (Table 3).

However, the evidence of spontaneity of the fluoride adsorption on hydrogel beads is obtained by calculating the standard Gibbs free energy (Table 1). The ΔG° of the adsorption process is -37.13 ± 0.02, -43.48 ± 0.02, and -43.07 ± 0.02 kJ mol^{-1} for PCZH, PZH, and PFZH. The high negative value of standard Gibbs free energy and the enthalpy indicates chemisorption of fluoride on hydrogel beads.[8,21,47] Hence, based on the column adsorption models, analysis of the breakthrough curves and the thermodynamics of adsorption, it is proved that the fluoride adsorption to the hydrogel beads occurs mainly by chemisorption.

3.5. Column Performance Indicator. The performance of the column is evaluated based on the degree of sorbent used (DoSU), sorbent usage rate (SUR), and the number of bed volumes processed.

The DoSU during the adsorption is the ratio of fluoride uptake at the breakthrough (q_b) to the fluoride uptake at equilibrium (q_e), which is given by the equation

$$\mathrm{DoSU} = \frac{q_b}{q_e} \tag{21}$$

In addition, the SUR is defined as the unit mass of the adsorbent (M in g) required to obtain a clean effluent before the breakthrough (V_b in L) which is given by

$$\mathrm{SUR} = \frac{M}{V_b} = \frac{M}{Qt_b} \tag{22}$$

Another, important parameter is the number of bed volumes processed by the column, which is given by the equation

$$\text{Number of bed volume} = \frac{\text{Volume treated at breakthrough}(V_b)}{\text{Volume of adsorbent bed}} \tag{24}$$

The higher value of DoSU indicates that the adsorbent used for column adsorption has good fluoride removal efficiency at the breakthrough. Similarly, a lower value of SUR implies that lesser amount of the adsorbent is required to treat contaminated water. The higher value of bed volumes signifies that the column can be used for the treatment of a larger volume of contaminated water.[48]

https://doi.org/10.1021/acsomega.2c00834
ACS Omega 2022, 7, 15048−15063

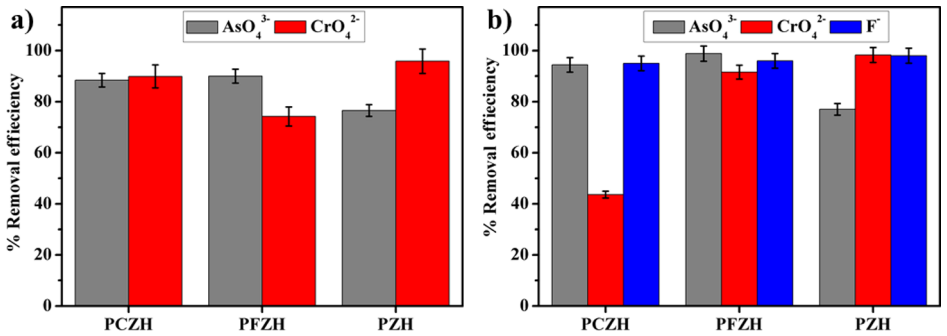

Figure 8. Removal of potentially toxic metal ions by the hydrogel beads from a solution containing: (a) only arsenate/chromate (volume = 10 mL) and (b) mixture of fluoride (volume = 5 mL), arsenate (volume = 5 mL), and chromate (volume = 5 mL).

The degree of sorbent usage is higher for the column of smaller bed height and lower flow rate. However, the degree of sorbent usage is enhanced for a column of greater bed height, even at a higher flow rate, as more adsorbent sites are available for adsorption. Among the hydrogel beads, PCZH exhibits the highest DoSU implying good fluoride removal efficiency before the breakthrough.

On increasing the bed height, the SUR decreases, which implies that a lower adsorbent dosage is required for obtaining clean water at a greater bed height. For PCZH, PZH, and PFZH beads, the SUR for a bed height of 8 cm is 0.85 ± 0.05, 2.18 ± 0.05, and 2.03 ± 0.05 g L^{-1}, while fluoride removal efficiencies are 74 ± 0.02%, 62 ± 0.02%, and 61 ± 0.02%, respectively (Tables 2 and 5). Moreover, the SUR are 1.58 ± 0.05 (PCZH), 1.43 ± 0.05 (PZH), and 1.67 ± 0.05 g L^{-1} (PFZH) at a flow rate of 1 mL min^{-1}, while a larger adsorbent dosage is required to treat 1 L of fluoride-containing water at a lower flow rate.

The number of treated bed volumes depends mainly on the flow rate of the fluoride solution. Increasing the column bed height at a constant flow rate does not bring about a drastic change in the treated bed volume. However, on the flow rate from 0.10 ± 0.01 to 1 ± 0.01 mL min^{-1} increases the number of processed bed volumes increase from 52.01 ± 0.10 to 214.83 ± 0.10 for PCZH, from 29.40 ± 0.10 to 237.44 ± 0.10 for PZH, and 59.93 ± 0.10 to 203.52 ± 0.10 for PFZH. The number of bed volumes processed by the column of PCZH with a bed height of 4 ± 0.2 cm at a flow rate of 1 ± 0.01 mL min^{-1} is the highest, which implies that PCZH could be used for treating a larger volume of water.

3.6. Adsorbent Regeneration. The economic viability of the adsorbent is determined by its reusability. In the column adsorption studies, the fixed-bed column is recharged by eluting with 0.10 ± 0.02 mol L^{-1} HCl for 2 ± 0.02 h at a flow rate of 1 ± 0.01 mL min^{-1} (Figure 6). PFZH retains 51 ± 0.02% efficiency, while PCZH and PZH have 54 ± 0.02% and 46 ± 0.02% fluoride removal efficiency after the third regeneration cycle (Table 6). This shows that fluoride adsorption in the continuous flow system might require a longer regeneration time. However, the calculated value of equilibrium adsorption capacity does not change significantly on reusing the hydrogel beads as the time required for the saturation of the column is less affected on regeneration (Table 6). This shows that the hydrogel beads have good regenerability.[18,49]

3.7. Practical Applicability of Metal−PVA Hydrogels for Water Treatment. The metal-incorporated hydrogel beads exhibit good selectivity toward fluoride. A simulated solution containing 10 ± 0.2 mg L^{-1} fluoride and 100 ± 0.2 mg L^{-1} of interfering ions such as nitrates, chlorides, phosphates, bicarbonates, and sulfates is fed into a column of 2 ± 0.2 cm bed height containing 0.90 ± 0.01 g of hydrogel beads maintained at a flow rate of 0.50 ± 0.01 mL min^{-1} (Figure 7c). Generally, these ions compete for the adsorbent sites and lower the fluoride removal efficiency of the adsorbent.[48,50] However, in the case of the hydrogel beads, the fluoride removal efficiency decreases marginally even in the presence of interfering ions. The fluoride removal efficiency is lowered by < 1 ± 0.02% in the simulated solution containing interfering ions when compared with a column subjected to a feed solution containing only 10 ± 0.20 mg L^{-1} fluoride (Tables 2 and 8). The fluoride removal capacity of the column follows the order: PZH (14.17 ± 0.05 mg g^{-1}) > PCZH (8.05 ± 0.05 mg g^{-1}) > PFZH (5.98 ± 0.05 mg g^{-1}). However, PCZH has good fluoride removal efficiency at the breakthrough as DoSU is the highest (62.77 ± 0.02%). This indicates that the column containing PCZH reduces the fluoride content of water containing interfering ions below the permissible limit for a longer duration. However, a slight decrease in the column breakthrough time, saturation time, and treated effluent volume is observed for all the hydrogel beads in the presence of interfering ions.

Furthermore, the efficiency of the fixed-bed column of PCZH, PZH, and PFZH is checked for its practical applicability by subjecting it to a continuous feed of the groundwater sample collected from the Anantapur district of Andhra Pradesh, India (Figure 5). The physico-chemical analysis of the groundwater is done before and after adsorption (Table 7). The concentrations of K^+, Mg^{2+}, Ca^{2+}, and Na^+ are estimated by microwave-assisted atomic emission spectroscopy (MP-AES 4200, Agilent, USA). The fixed-bed column adsorption of fluoride by the hydrogel beads shows promising results (Tables 7−9). About 57 ± 0.02% of fluoride is removed from the groundwater by PZH beads. The degree of sorbent usage is 86 ± 0.02% for PZH, while it is 77 ± 0.02% and 61 ± 0.02% for PCZH and PFZH beads which implies that the column could be used effectively for defluoridation of groundwater (Table 9).

Mathematical models (Thomas, Bohart−Adams, and Yoon−Nelson) are used for the analysis of the breakthrough curve (Figure 7d). The equilibrium fluoride capacity calculated from the Thomas model is well correlated with the results obtained from the fixed-bed column adsorption studies (Table 10). The time required for 50% saturation of the column is PZH (48 ± 0.02 h) > PCZH (41 ± 0.02 h) > PFZH (14 ± 0.02 h). Likewise, the saturation concentration

https://doi.org/10.1021/acsomega.2c00834
ACS Omega 2022, 7, 15048−15063

Table 11. Comparison of the Performance of the Adsorbents Reported in Literature for Fixed-Bed Fluoride Adsorption Studies with the Current Work[a]

material	pH	column exhaustion time	initial $[F^-]$ (mg L^{-1})	flow rate (mL min^{-1})	bed height (cm)	regeneration efficiency	q_0 (mg g^{-1})	real-time sample analysis by fixed-bed column	ref.
kanuma mud	5−7	80 h	20	5	10	32% loss in efficiency after three regeneration cycles; regenerating agent: 0.1 mol L^{-1} of NaOH	1.59	not reported	12
rGO/ZrO_2	7	∼84 h	25	1.66	7.5	negligible loss in efficiency after the third cycle; regenerating agent: 10% NaOH	45.70	not reported	17
magnesia-pollulan	4	NA*	10	16	20	could be restored to 97% of its original capacity only by calcination at 500 °C.	16.60	not reported	51
xanthate-modified *Ficus religiosa*	NA*	375 min	50	2	30	25% loss in efficiency after the second cycle; regenerating agent: 0.1 mol L^{-1} of NaOH	19.72	not reported	14
Tinospora cordifolia	7	39 h	5	13	36	16% loss in efficiency after the third cycle; regenerating agent: 0.1 mol L^{-1} of NaOH;	3.88	not reported	52
okra stem biochar	2	not reported	5	4	8	not reported	6.00	not reported	7
PCZH	6.5	79 h,	10	1	4	9%, 12%, and 4% loss in efficiency after the third regeneration cycle; regenerating agent: 0.1 mol L^{-1} HCl	25.66,	48%	the current study
PZH		135 h,					38.17,	57%	
PFZH		56 h					13.75	40% removal from the ground water sample with a fluoride feed concentration of 2.84 mg L^{-1}	

[a]*NA = Data not available.

also follows a similar trend, PZH (61.87 ± 0.05 mg L^{-1}) > PCZH (53.59 ± 0.05 mg L^{-1}) > PFZH (18.70 ± 0.05 mg L^{-1}). Thus, the hydrogel beads have good fluoride removal capacity from alkaline groundwater containing high total dissolved salts (Table 10).

Furthermore, the efficacy of the hydrogel beads for the removal of other anionic contaminants such as arsenate and chromate is also tested in batch adsorption studies. The ingestion of these potentially toxic metal ions cause organ failure and can be fatal.[19,20] Therefore, the hydrogel beads are used as adsorbents for the removal of arsenate and chromate from 100 ± 0.2 mg L^{-1} solution of these ions. The residual concentration of As (V) and Cr (VI) ions present in the solution are estimated by microwave-assisted atomic emission spectroscopy. About 90 ± 0.02%, 88 ± 0.02%, and 77 ± 0.02% of arsenate and 74 ± 0.02%, 90 ± 0.02%, and 96 ± 0.02% of chromate is removed by PFZH, PCZH, and PZH, respectively (Figure 8a). The ability of the hydrogel beads to simultaneously adsorb these contaminants is determined by immersing 0.18 ± 0.02 g of hydrogel beads in a solution containing 10 ± 0.2 mg L^{-1} of F^-, and 100 ± 0.2 mg L^{-1} of $AsO_4^{3-}$and CrO_4^{2-}. All the hydrogel beads are efficient in bringing about instantaneous removal of contaminants (Figure 8b). PFZH exhibits excellent removal efficiencies of 99 ± 0.02% (CrO_4^{2-}), 92 ± 0.02% (AsO_4^{3-}), and 96 ± 0.02% (F^-). This shows that the hydrogels have multifarious applications in water treatment.

3.8. Comparative Assessment of Fluoride Adsorbents for Fixed-Bed Column Studies. Polyvinyl alcohol is an environmentally benign and economically viable polymer. Metal ions and glutaraldehyde are reacted with PVA to obtain self-assembled hydrogel beads by one-pot synthesis.[18] The metal−PVA hydrogel beads are more efficient in bringing about defluoridation of water when compared to the other adsorbents, which are used for fixed-bed adsorption studies, as reported in the literature (Table 11). These hydrogel beads remove fluoride at a wide pH range of 3−9, while most of the adsorbents exhibit good defluoridation capacity only at acidic pH.[7,18,51] Moreover, the metal ions are bound to the PVA matrix, which prevents secondary contamination of the treated water (Table 1).[18] The fixed-bed column of bio-based adsorbents have shown good fluoride removal efficiency from solutions containing higher initial fluoride concentrations. These adsorbents remove fluoride effectively at a greater flow rate. However, the adsorbents reported in literature have been used only for the removal of fluoride from simulated water samples (Table 11). Because the fixed-bed columns of metal−PVA hydrogel beads are used at a lower flow rate of 1 mL min^{-1}, the columns have a high exhaustion time for a bed height of 4 cm. Moreover, the fixed-bed columns of metal−PVA hydrogel beads are also effective in the removal of fluoride from alkaline groundwater. This proves that metal−PVA hydrogel beads can be used for the defluoridation of groundwater.

4. CONCLUSIONS

Defluoridation by a continuous-flow fixed-bed column of PCZH, PZH, and PFZH indicate that the hydrogel beads could be used to develop potent fluoride filters. The breakthrough time of the column nearly tripled on increasing the adsorbent bed height from 2 ± 0.2 to 8 ± 0.2 cm at a constant flow rate. The hydrogel beads have a good fluoride removal efficiency [PCZH (74 ± 0.02%), PFZH (61 ±

https://doi.org/10.1021/acsomega.2c00834
ACS Omega 2022, 7, 15048−15063

0.02%), and PZH (58 ± 0.02%)] when subjected to a continuous feed of 10 ± 0.2 mg L^{-1} fluoride concentration. The parameters obtained by fitting the breakthrough curves in Thomas, Bohart−Adams, and Yoon−Nelson models indicate that chemisorption predominates the adsorption process in the fixed-bed column. The fixed-bed column of hydrogel beads (bed height = 2 ± 0.2 cm) has good fluoride removal capacities of 8.05 ± 0.05, 14.17 ± 0.05, and 5.98 ± 0.05 mg g^{-1} for PCZH, PZH, and PFZH, respectively, from a 10 ± 0.20 mg L^{-1} fluoride solution containing interfering ions such as nitrates, bicarbonates, sulfates, phosphates, and chlorides. Thus, the hydrogel beads exhibit good selectivity toward fluoride. Additionally, the column of hydrogel beads effectively removes fluoride even from the groundwater sample and has good reusability. Moreover, PFZH exhibits removal efficiencies of 99 ± 0.02% (CrO_4^{2-}), 92 ± 0.02% (AsO_4^{3-}), and 96 ± 0.02% (F^-) from a solution containing 100 ± 0.2 mg L^{-1} of chromate and arsenate ions and 10 ± 0.2 mg L^{-1} of fluoride ions in batch adsorption studies. This indicates that these metal-complexed hydrogel beads have the ability to simultaneously remove arsenate, chromate, and fluoride anions from water and have potential industrial applications.

AUTHOR INFORMATION

Corresponding Author

Rajni Bhandari − *Department of Chemistry, Sri Sathya Sai Institute of Higher Learning, Anantapur 515001, India;* orcid.org/0000-0003-4894-3238; Phone: +91 9490044014; Email: rajnibhandari@sssihl.edu.in

Author

Sai Kiran Mani − *Department of Chemistry, Sri Sathya Sai Institute of Higher Learning, Anantapur 515001, India*

Complete contact information is available at: https://pubs.acs.org/10.1021/acsomega.2c00834

Notes

The authors declare no competing financial interest.

ACKNOWLEDGMENTS

The authors would like to express their gratitude to Sri Sathya Sai Institute of Higher Learning, Prasanthi Nilayam for the Central Research Instrumentation Facility (CRIF) and Central Research Laboratory (CRL), Anantapur Campus for providing the infrastructure to carry out the research work. S.K.M. acknowledges DST-INSPIRE for the doctoral fellowship (IF180553).

REFERENCES

(1) Ali, S.; Fakhri, Y.; Golbini, M.; Thakur, S. K.; Alinejad, A.; Parseh, I.; Shekhar, S.; Bhattacharya, P. Concentration of Fluoride in Groundwater of India : A Systematic Review, Meta-Analysis and Risk Assessment. *Groundw. Sustain. Dev.* **2019**, *9*, 100224.

(2) Samal, A. K.; Mishra, P. K.; Biswas, A. Assessment of Origin and Distribution of Fluoride Contamination in Groundwater Using an Isotopic Signature from a Part of the Indo-Gangetic Plain (IGP), India. *HydroResearch* **2020**, *3*, 75−84.

(3) Mani, S. K.; Bhandari, R.; Nehra, A.; Manohar, C. S.; Belliraj, S. K. Zirconium−Cerium and Zirconium−Lanthanum Complexed Polyvinyl Alcohol Films for Efficient Fluoride Removal from Aqueous Solution. *J. Dispersion Sci. Technol.* **2021**, *42*, 1−16.

(4) Sunitha, V.; Sudharshan Reddy, Y. Hydrogeochemical Evaluation of Groundwater in and around Lakkireddipalli and Ramapuram, Y.S.R District, Andhra Pradesh. *HydroResearch* **2019**, *2*, 85−96.

(5) Dhillon, A.; Kumar, D. Development of a Nanoporous Adsorbent for the Removal of Health-Hazardous Fluoride Ions from Aqueous Systems. *J. Mater. Chem. A* **2015**, *3*, 4215−4228.

(6) Dhillon, A.; Soni, S. K.; Kumar, D. Enhanced Fluoride Removal Performance by Ce − Zn Binary Metal Oxide : Adsorption Characteristics and Mechanism. *J. Fluorine Chem.* **2017**, *199*, 67−76.

(7) Kumar, H.; Patel, M.; Mohan, D. Simplified Batch and Fixed-Bed Design System for Efficient and Sustainable Fluoride Removal from Water Using Slow Pyrolyzed Okra Stem and Black Gram Straw Biochars. *ACS Omega* **2019**, *4*, 19513−19525.

(8) Loganathan, P.; Vigneswaran, S.; Kandasamy, J.; Naidu, R. Defluoridation of Drinking Water Using Adsorption Processes. *J. Hazard. Mater.* **2013**, *248-249*, 1−19.

(9) Patel, H. Fixed-Bed Column Adsorption Study: A Comprehensive Review. *Appl. Water Sci.* **2019**, *9*, 1−17.

(10) Xu, Z.; Cai, J.-g.; Pan, B.-c. Mathematically Modeling Fixed-Bed Adsorption in Aqueous Systems. *J. Zhejiang Univ., Sci., A* **2013**, *14*, 155−176.

(11) Askari, M.; Salehi, E.; Ebrahimi, M.; Barati, A. Application of Breakthrough Curve Analysis and Response Surface Methodology for Optimization of a Hybrid Separation System Consisting of Fixed-Bed Column Adsorption and Dead-End Depth Filtration. *Chem. Eng. Process.* **2019**, *143*, 107594.

(12) Chen, N.; Zhang, Z.; Feng, C.; Li, M.; Chen, R.; Sugiura, N. Investigations on the Batch and Fixed-Bed Column Performance of Fluoride Adsorption by Kanuma Mud. *Desalination* **2011**, *268*, 76−82.

(13) Sarkar, M.; Banerjee, A.; Pramanick, P. P.; Sarkar, A. R. Design and Operation of Fixed Bed Laterite Column for the Removal of Fluoride from Water. *Chem. Eng. J.* **2007**, *131*, 329−335.

(14) Tariq, M.; Farooq, U.; Athar, M.; Salman, M.; Tariq, M.; Shahida, S.; Farooqi, Z. H. Fluoride Removal Using Simple Protonated and Xanthate Modified Protonated Ficus Religiosa Branch Powder in a Fixed-Bed Column. *Desalin. Water Treat.* **2019**, *150*, 204−212.

(15) Paudyal, H.; Pangeni, B.; Inoue, K.; Kawakita, H.; Ohto, K.; Alam, S. Adsorptive Removal of Fluoride from Aqueous Medium Using a Fixed Bed Column Packed with Zr (IV) Loaded Dried Orange Juice Residue. *Bioresour. Technol.* **2013**, *146*, 713−720.

(16) Ghorai, S.; Pant, K. K. Investigations on the Column Performance of Fluoride Adsorption by Activated Alumina in a Fixed-Bed. *Chem. Eng. J.* **2004**, *98*, 165−173.

(17) Mohan, S.; Singh, D. K.; Kumar, V.; Hasan, S. H. Effective Removal of Fluoride Ions by RGO/ZrO2 Nanocomposite from Aqueous Solution: Fixed Bed Column Adsorption Modelling and Its Adsorption Mechanism. *J. Fluorine Chem.* **2017**, *194*, 40−50.

(18) Mani, S. K.; Bhandari, R.; Nehra, A. Self-Assembled Cylindrical Zr (IV), Fe (III) and Cu (II) Impregnated Polyvinyl Alcohol-Based Hydrogel Beads for Real-Time Application in Fluoride Removal. *Colloids Surf., A* **2021**, *610*, 125751.

(19) Andjelkovic, I.; Tran, D. N. H.; Kabiri, S.; Azari, S.; Markovic, M.; Losic, D. Graphene Aerogels Decorated with α - FeOOH Nanoparticles for Efficient Adsorption of Arsenic from Contaminated Waters. *ACS Appl. Mater. Interfaces* **2015**, *7*, 9758−9766.

(20) Rajak, J. K.; Khandelwal, N.; Behera, M. P.; Tiwari, E.; Singh, N.; Ganie, Z. A.; Darbha, G. K.; Abdolahpur Monikh, F.; Schäfer, T. Removal of Chromate Ions from Leachate-Contaminated Groundwater Samples of Khan Chandpur, India, Using Chitin Modified Iron-Enriched Hydroxyapatite Nanocomposite. *Environ. Sci. Pollut. Res.* **2021**, *28*, 41760−41771.

(21) Patel, H. Comparison of Batch and Fixed Bed Column Adsorption: A Critical Review. *Int. J. Environ. Sci. Technol.* **2021**, 1−18.

(22) Tran, H. N.; You, S.-J.; Hosseini-bandegharaei, A.; Chao, H.-P. Mistakes and Inconsistencies Regarding Adsorption of Contaminants from Aqueous Solutions : A Critical Review. *Water Res.* **2017**, *120*, 88−116.

(23) Chatterjee, A.; Schiewer, S. Biosorption of Cadmium(II) Ions by Citrus Peels in a Packed Bed Column: Effect of Process Parameters and Comparison of Different Breakthrough Curve Models. *Clean: Soil, Air, Water* **2011**, *39*, 874−881.
(24) Water Environment Federation, American Public Health Association. *Standard Methods for the Examination of Water and Wastewater*, 19th ed.; Greenberg, A. E., Ed.; American Public Health Association: Washington DC, USA, 1995; Vol. *142*.
(25) Han, R.; Wang, Y.; Zhao, X.; Wang, Y.; Xie, F.; Cheng, J.; Tang, M. Adsorption of Methylene Blue by Phoenix Tree Leaf Powder in a Fixed-Bed Column : Experiments and Prediction of Breakthrough Curves. *Desalination* **2009**, *245*, 284−297.
(26) Rout, P. R.; Bhunia, P.; Dash, R. R. Evaluation of Kinetic and Statistical Models for Predicting Breakthrough Curves of Phosphate Removal Using Dolochar-Packed Columns. *J. Water Process. Eng.* **2017**, *17*, 168−180.
(27) Song, W.; Xu, X.; Tan, X.; Wang, Y.; Ling, J.; Gao, B.; Yue, Q. Column Adsorption of Perchlorate by Amine-Crosslinked Biopolymer Based Resin and Its Biological, Chemical Regeneration Properties. *Carbohydr. Polym.* **2015**, *115*, 432−438.
(28) Patel, H. Batch and Continuous Fixed Bed Adsorption of Heavy Metals Removal Using Activated Charcoal from Neem (Azadirachta Indica) Leaf Powder. *Sci. Rep.* **2020**, *10*, 16895.
(29) Naja, G.; Volesky, B. Behavior of the Mass Transfer Zone in a Biosorption Column. *Environ. Sci. Technol.* **2006**, *40*, 3996−4003.
(30) Rangabhashiyam, S.; Nandagopal, M. S. G.; Nakkeeran, E.; Selvaraju, N. Adsorption of Hexavalent Chromium from Synthetic and Electroplating Effluent on Chemically Modified Swietenia Mahagoni Shell in a Packed Bed Column. *Environ. Monit. Assess.* **2016**, *188*, 411.
(31) Chu, K. H. Breakthrough Curve Analysis by Simplistic Models of Fixed Bed Adsorption : In Defense of the Century-Old Bohart-Adams Model. *Chem. Eng. J.* **2020**, *380*, 122513.
(32) Choy, K. K. H.; Ko, D. C. K.; Cheung, C. W.; Porter, J. F.; McKay, G. Film and Intraparticle Mass Transfer during the Adsorption of Metal Ions onto Bone Char. *J. Colloid Interface Sci.* **2004**, *271*, 284−295.
(33) Pervez, M. N.; Stylios, G. K.; Liang, Y.; Ouyang, F.; Cai, Y. Low-Temperature Synthesis of Novel Polyvinylalcohol (PVA) Nanofibrous Membranes for Catalytic Dye Degradation. *J. Cleaner Prod.* **2020**, *262*, 121301.
(34) Velazquez-jimenez, L. H.; Hurt, R. H.; Matos, J.; Rangel-mendez, J. R. Zirconium − Carbon Hybrid Sorbent for Removal of Fluoride from Water : Oxalic Acid Mediated Zr (IV) Assembly and Adsorption Mechanism. *Environ. Sci. Technol.* **2014**, *48*, 1166−1174.
(35) Chandrakala, H. N.; Ramaraj, B.; Shivakumaraiah, G. M.; Madhu, G. M.; Siddaramaiah. Preparation of Polyvinyl Alcohol − Lithium Zirconate Nanocomposite Films and Analysis of Transmission , Absorption, Emission Features, and Electrical Properties. *J. Phys. Chem. C* **2013**, *117*, 4771−4781.
(36) Maity, N.; Barman, S.; Minenkov, Y.; Ould-Chikh, S.; Abou-Hamad, E.; Ma, T.; Qureshi, Z. S.; Cavallo, L.; D'Elia, V.; Gates, B. C.; Basset, J.-M. A Silica-Supported Monoalkylated Tungsten Dioxo Complex Catalyst for Olefin Metathesis. *ACS Catal.* **2018**, *8*, 2715−2729.
(37) Maity, N.; Barman, S.; Abou-Hamad, E.; D'Elia, V.; Basset, J.-M. Clean Chlorination of Silica Surfaces by a Single-Site Substitution Approach. *Dalton Trans.* **2018**, *47*, 4301−4306.
(38) Zhang, H.; Zhang, J. The Preparation of Novel Polyvinyl Alcohol (PVA)-Based Nanoparticle/Carbon Nanotubes (PNP/CNTs) Aerogel for Solvents Adsorption Application. *J. Colloid Interface Sci.* **2020**, *569*, 254−266.
(39) Figueiredo, K. C. S.; Alves, T. L. M.; Borges, C. P. Poly (Vinyl Alcohol) Films Crosslinked by Glutaraldehyde Under Mild Conditions. *J. Appl. Polym. Sci.* **2008**, *111*, 3074−3080.
(40) An, Y.; Han, W.; Han, J.; Zhao, G.; Zhou, S.; Zhang, X. Synergistic Effect on the Mechanical Behaviors of Ternary Graphene Oxide-Zirconium Diboride-Poly (Vinyl Alcohol) Papers. *Mater. Des.* **2016**, *112*, 275−281.
(41) Togashi, T.; Naka, T.; Asahina, S.; Sato, K.; Takami, S.; Adschiri, T. Surfactant-Assisted One-Pot Synthesis of Superparamagnetic Magnetite Nanoparticle Clusters with a Tunable Cluster Size and Sensitivity for Magnetic Field. *Dalton Trans.* **2011**, *40*, 1073−1078.
(42) Patel, S. B.; Baker, N.; Marques, I.; Hamlekhan, A.; Mathew, M. T.; Takoudis, C.; Friedrich, C.; Sukotjo, C.; Shokuhfar, T. Transparent TiO2 Nanotubes on Zirconia for Biomedical Applications. *RSC Adv.* **2017**, *7*, 30397−30410.
(43) Gong, J.; Luo, L.; Yu, S.-H.; Qian, H.; Fei, L. Synthesis of Copper/Cross-Linked Poly(Vinyl Alcohol) (PVA) Nanocables via a Simple Hydrothermal Route. *J. Mater. Chem.* **2006**, *16*, 101−105.
(44) Elango, M.; Deepa, M.; Subramanian, R.; Mohamed Musthafa, A. Synthesis, Characterization, and Antibacterial Activity of Polyindole/Ag−Cuo Nanocomposites by Reflux Condensation Method. *Polym.-Plast. Technol. Eng.* **2018**, *57*, 1440−1451.
(45) Dou, X.; Mohan, D.; Pittman, C. U.; Yang, S. Remediating Fluoride from Water Using Hydrous Zirconium Oxide. *Chem. Eng. J.* **2012**, *198-199*, 236−245.
(46) McCabe, W. L.; Smith, J. C.; Peter, H. *Unit Operations of Chemical Engineering*, 6th ed.; McGraw-Hill International Ed: New York, 2001.
(47) Mani, S. K.; V, P.; Bhandari, R. Experimental and Computational Investigation of Divalent, Trivalent, and Tetravalent Metal Ion Complexes of Polyvinyl Alcohol as Adsorbents for Fluoride Remediation. *J. Mol. Struct.* **2022**, *1252*, 132139.
(48) Mudzielwana, R.; Gitari, M. W. Removal of Fluoride from Groundwater Using MnO2 Bentonite-Smectite Rich Clay Soils Composite. *Groundw. Sustain. Dev.* **2021**, *14*, 100623.
(49) Dharmapriya, T. N.; Lee, D.-Y.; Huang, P.-J. Novel Reusable Hydrogel Adsorbents for Precious Metal Recycle. *Sci. Rep.* **2021**, *11*, 19577.
(50) Dong, S.; Wang, Y. Characterization and Adsorption Properties of a Lanthanum-Loaded Magnetic Cationic Hydrogel Composite for Fluoride Removal. *Water Res.* **2016**, *88*, 852−860.
(51) Ye, Y.; Yang, J.; Jiang, W.; Kang, J.; Hu, Y.; Ngo, H. H.; Guo, W.; Liu, Y. Fluoride Removal from Water Using a Magnesia-Pullulan Composite in a Continuous Fixed-Bed Column. *J. Environ. Manage.* **2018**, *206*, 929−937.
(52) Chakraborty, M.; Pandey, M.; Pandey, P. Fixed Bed Column Performance of Tinospora Cordifolia for Defluoridation of Water. *Water Supply* **2021**, *21*, 2324−2332.

https://doi.org/10.1021/acsomega.2c00834
ACS Omega 2022, 7, 15048−15063